4.5 RECENT PROGRESS OF CRACK BRIDGING MODELING OF DUCTILE-PHASE-TOUGHENED W-Cu COMPOSITES – W. Setyawan, C. H. Henager, Jr., K. B. Wagner, T. J. Roosendaal, B. A. Borlaug, and R. J. Kurtz (Pacific Northwest National Laboratory); G. R. Odette, K. H. Cunningham, and F. W. Zok (University of California, Santa Barbara)

OBJECTIVE

The objective of this study is to develop the materials science of ductile-phase W-composites for plasma-facing components in fusion reactors. Parametric study of a bridging model for W-Cu is discussed.

SUMMARY

A crack bridging model using calculated Cu stress-strain curves has been developed to study the toughening of W-Cu composites. A strengthening factor and necking parameters have been added to the model for the ductile-phase bridges to incorporate constraint effects at small bridge sizes. Parametric studies are performed to investigate the effect of these parameters. The calculated maximum applied stress intensity, a_{Kmax}, to induce a 1-mm stable crack is compared to the experimental stress intensity at peak load, K_{peak}. Without bridge necking, increasing the strengthening factor improves the agreement between a_{Kmax} and K_{peak} when plotted vs. logarithm of the displacement rate. Improvement can also be achieved by allowing necking with a larger failure strain. While the slope is better matched with this latter approach, the calculated value of a_{Kmax} is significantly larger than K_{peak}.

PROGRESS AND STATUS

Updated Results

In our previous report [1], the conversion of the displacement rate to strain rate was incorrect. In this report, we update the crack-bridging model using the corrected strain rate data. In addition, we include the effect of bridge necking. The 3-point bending specimen has a span L = 16.05 mm, a height w = 3.3 mm, and a thickness b = 1.67 mm. The experimental midpoint displacement rates, $\dot{\delta}$, were converted into a tensile strain rate, $\dot{\varepsilon}$, using the following 3-point bending formula [2],

$$\dot{\epsilon} = \frac{2w(n+2)}{L^2}\dot{\delta} \tag{1}$$

where n is the stress exponent for creep (n = 1 for elastic bending). Note that n depends on $\dot{\varepsilon}$ and does not correspond to the exponent appearing in the Dorn equation. The conversion is performed until the displacement rate converges to the experimental value within 1% relative error (see Table 1).

To compare model results to experimental data, an equivalent dataset was considered. The model begins by considering an initial applied K, a_{K0}, and a_0/w, where a_0 is the initial crack length. For the case treated here, a_0 was 0.7 mm and w was 3.3 mm. A bridge radius of 5 µm was assumed with a Cu volume fraction of 0.4 to match previous SEM data on Cu area fraction in polished cross-sections. The bridges are uniformly distributed according to the volume fraction with the first one at 0.02 mm from a_0. The Young's modulus for W at 293, 679, and 905 K is 410, 393, and 385 GPa, respectively, and for Cu is 130, 110, and 95, respectively. The Young's modulus of the composite was taken as the average value based on the volume fraction.

Table 1. Conversion of the midpoint displacement rate, $\dot{\delta}$, measured in experiments to the tensile strain rate, $\dot{\varepsilon}$, for the flow stress model of Cu [1].

T (K)	$\dot{\delta}$ (mm/min)	$\dot{\varepsilon}$ (1/s)	n	c_L	σ_y (MPa)	σ_{ulteng} (MPa)	ε_{ulteng}
293	2.0	1.178e-1	135.900	33.75	79.5	209.9	0.2612
	0.2	1.139e-2	131.300	34.37	78.2	206.2	0.2611
	0.02	1.100e-3	126.700	34.98	76.7	202.5	0.2612
	0.002	1.061e-4	122.100	35.60	75.1	198.7	0.2614
	0.0002	1.022e-5	117.460	36.23	73.3	194.8	0.2618
679	2.0	3.884e-2	43.198	36.47	74.9	175.4	0.2496
	0.2	3.497e-3	38.637	38.49	69.8	165.1	0.2507
	0.02	3.113e-4	34.101	40.56	63.6	154.4	0.2534
	0.002	2.697e-5	29.582	42.67	56.0	142.8	0.2581
	0.0002	2.294e-6	24.857	45.01	46.5	129.7	0.2658
905	2.0	2.349e-2	25.470	40.53	71.8	151.1	0.2375
	0.2	1.967e-3	20.997	44.33	62.4	135.3	0.2411
	0.02	1.596e-4	16.638	48.33	50.2	117.9	0.2500
	0.002	1.240e-5	12.393	52.98	35.0	98.1	0.2662
	0.0002	9.128e-7	8.688	59.74	19.3	76.7	0.2890

In the model, the crack growth was simulated under constant load. The criteria for crack growth was a_{Kcrit} = 8 MPa√m so that a crack will arrest when a_{Ktip} falls below 8 MPa√m. The maximum applied K (a_{Kmax}) was determined for each temperature and strain rate for which the crack was still bridged and stable after 1-mm of crack growth. Determining a_{Kmax} for which crack arrest will still occur is roughly equivalent to measuring the peak load stress intensity, K_{peak}, in the experiments, and allows for a direct comparison of datasets, one experimental and one simulated. In addition to recording a_{Kmax}, other calculated values were recorded as well: a_{Ktip} and the difference between a_{Kmax} and a_{Ktip}, denoted as ΔK, which represents the total closure force due to the bridges, or the net toughening due to the bridges.

A strengthening factor, *sfact*, is introduced into the model to account for bridge size effects and tri-axial constraint. This factor linearly scales the stress strain curve to account for these effects that can act to greatly increase the fracture strength of small, constrained bridges. In this approach, stress in the stress-strain curve is multiplied by *sfact* while the strain is unchanged. The value of *sfact* is determined as the strengthening factor needed to arrest a 1-mm crack at 905 K ($2/3T_m$) with a displacement rate of 0.0002 mm/min. We arbitrarily take the value obtained using the smallest applied load. The resulting *sfact* is 3.9. This value is then used for other temperatures and strain rates.

Using *sfact* = 3.9, the value of a_{Kmax} is then determined. The results are shown in Table 2. The value of a_{Kmax} is typically larger than K_{peak}. Note that within a 1-mm crack there are 40 bridges. From Table 2 we see that the number of bridges is less than 40. However, if we increase the applied K, the crack becomes unstable. Figure 1a plots a_{Kmax} and K_{peak} as a function of displacement rate. In Fig. 1a, a single-value shift has been applied to the a_{Kmax} data so that at 679 K ($1/2T_m$) and 0.0002 mm/min the value matches K_{peak}. In this case, the shift is 14.5-18.3 = -3.8 MPa√m. The shift allows for a more convenient comparison between model and experimental data. The best match is obtained at the intermediate temperature ($1/2T_m$). We varied *sfact* to explore its effects and with *sfact* = 8 (Fig. 1b) the match of room-temperature (*RT*) and $1/2T_m$ curves are improved. However, the curve at $2/3T_m$ is less sensitive to *sfact* changes.

Table 2. Model results showing computed values of critical parameters for stable bridged cracks with *sfact* = 3.9.

Temp (K)	Displ. Rate (mm/min)	Strain Rate (1/s)	# bridges	ΔK (MPa√m)	a_{Kmax} (MPa√m)	Exp. K_{peak} (MPa√m)
293	2	1.178e-1	23	15.1	22.9	23.5
293	0.2	1.139e-2	23	14.8	22.7	23.7
293	0.02	1.100e-3	23	14.5	22.4	21.3
293	0.002	1.061e-4	23	14.2	22.1	19.6
293	0.0002	1.022e-5	23	13.8	21.8	20.5
679	2	3.884e-2	22	12.1	20.0	17.6
679	0.2	3.497e-3	22	11.3	19.1	17.0
679	0.02	3.113e-4	23	11.2	19.2	15.2
679	0.002	2.697e-5	25	11.2	19.1	15.2
679	0.0002	2.294e-6	26	10.4	18.3	14.5
905	2	2.349e-2	21	10.2	18.2	13.5
905	0.2	1.967e-3	23	10.1	17.9	11.3
905	0.02	1.596e-4	25	9.4	17.3	9.4
905	0.002	1.240e-5	27	8.2	16.2	8.6
905	0.0002	9.128e-7	31	7.2	15.2	4.9

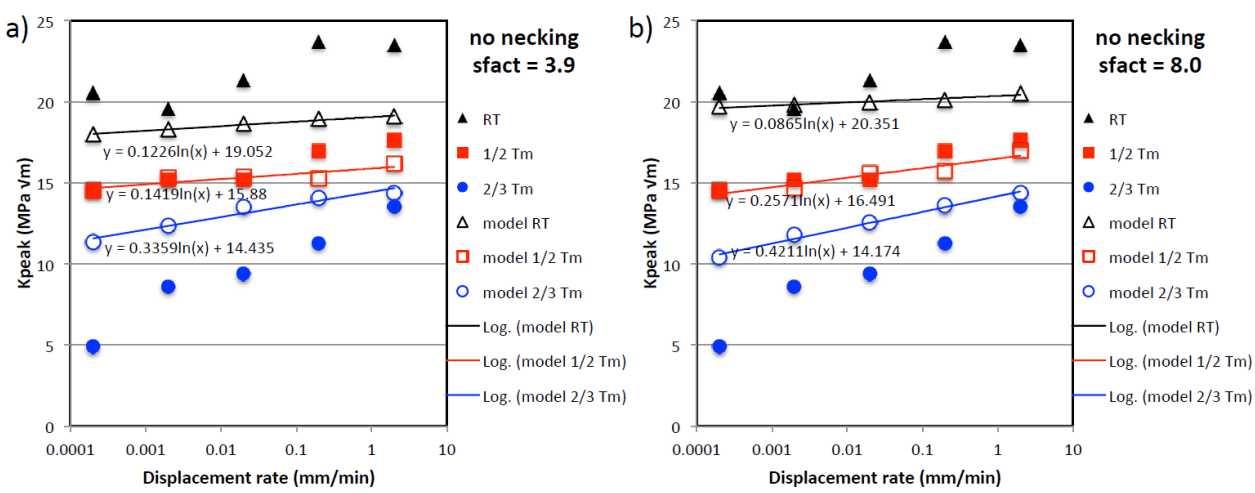

Figure 1. Experimental K_{peak} (filled symbols) and computed a_{Kmax} (open symbols) for W-Cu bridge model vs. displacement rate at room temperature (*RT*), 679 K (*1/2T$_m$*), and 905 K (*2/3T$_m$*). A shift of -3.8 and -9.8 MPa√m is applied to a_{Kmax} data in a) and b) respectively.

We have added a new capability in the crack bridging model to include necking of the bridges before failure. At this moment, we take the necking model from [3] as follows:

$$y(x) = \sqrt{x}\left[e^{\left(1-x^{(c+1)/2}\right)}\right]^{1/(c+1)} \tag{2}$$

where $x = \varepsilon/\varepsilon_{ulteng}$ and $y = \sigma/\sigma_{ulteng}$. Necking is applied when $\varepsilon > \varepsilon_{ulteng}$. Figure 2 illustrates the necking curve for several values of *c*.

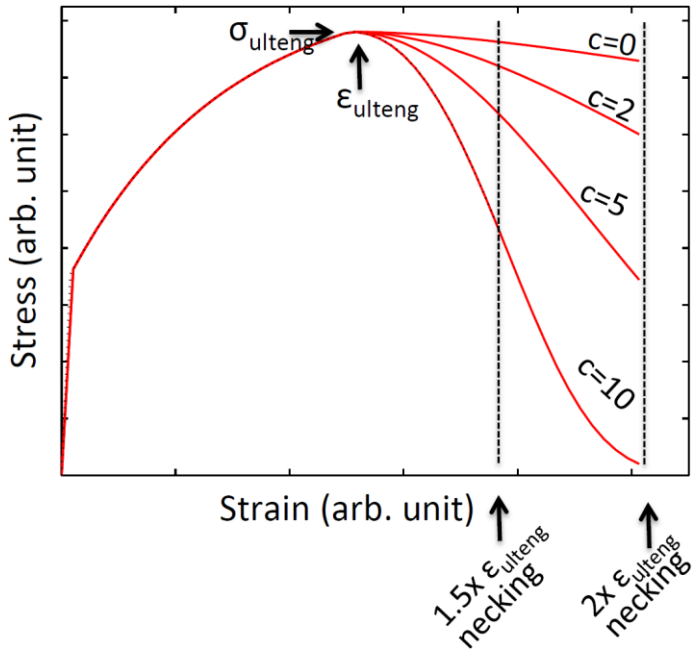

Figure 2. Illustration of the necking model for different values of *c*. Necking occurs when the strain is larger than the ultimate engineering strain, ε_{ulteng}.

To investigate the toughening behavior when necking is taken into account, we use *sfact* = 3.9 data and necking parameter c = 5 and vary the necking extension factor up to 2x. An extension factor of 2x necking denotes a failure strain of $\varepsilon_{fail} = 2\varepsilon_{ulteng}$. Table 3 summarizes the results for the 2x necking. Figure 3a shows the a_{kmax} plot with a shift of -6.3 MPa√m. Compared to Fig. 1a, necking improves the slope match of the *RT* and $1/2T_m$ curves. Note that 1.5x necking (not shown) yields very similar curves as the 2x necking. Next, with *sfact* = 3.9 and 2x necking, we simulate with a necking parameter *c* of 0, 2, 5, and 10. The data with *c* = 2 is presented in Table 4 and is plotted in Fig. 3b with a shift of -8.5 MPa√m. Reducing the value of *c* from 5 to 2 appears to improve the slope match for the $2/3T_m$ curve. Further improvement of the slope match at $2/3T_m$ can be obtained with a lower value of *c*, e.g. *c* = 0 as shown in Figure 4. In Fig. 4, a shift of -12.5 MPa√m has been applied to a_{Kmax}.

Table 3. Model results showing computed values of critical parameters for stable bridged cracks with *sfact* = 3.9 and necking condition of $\varepsilon_{fail} = 2\varepsilon_{ulteng}$ with *c* = 5. Maximum necking denotes the ratio of the maximum strain with ε_{ulteng} of the most stretched bridge.

Temp (K)	Displ. Rate (mm/min)	# bridges	# necking bridges	max. necking	ΔK (MPa√m)	a_{Kmax} (MPa√m)
293	2	26	6	1.25	17.9	25.8
293	0.2	26	6	1.25	17.5	25.5
293	0.02	27	7	1.49	18.1	25.7
293	0.002	27	7	1.72	17.8	25.7
293	0.0002	27	6	1.26	17.4	25.3
679	2	26	6	1.27	15.2	23.2
679	0.2	27	7	1.75	15.0	22.8
679	0.02	27	6	1.23	13.9	21.8
679	0.002	29	7	1.91	13.9	21.8
679	0.0002	30	6	1.25	13.0	20.8
905	2	26	7	1.60	13.3	21.2
905	0.2	27	7	1.26	12.4	20.4
905	0.02	29	7	1.22	11.6	19.5
905	0.002	32	7	1.25	10.7	18.7
905	0.0002	37	9	1.49	10.0	18.0

Table 4. Model results showing computed values of critical parameters for stable bridged cracks with *sfact* = 3.9 and necking condition of $\varepsilon_{fail} = 2\varepsilon_{ulteng}$ with *c* = 2. Maximum necking denotes the ratio of the maximum strain with ε_{ulteng} of the most stretched bridge.

Temp (K)	Displ. Rate (mm/min)	# bridges	# necking bridges	max. necking	ΔK (MPa√m)	a_{Kmax} (MPa√m)
293	2	28	10	1.69	19.9	27.9
293	0.2	28	10	1.66	19.6	27.6
293	0.02	29	11	2.00	20.0	27.9
293	0.002	29	11	1.73	19.6	27.5
293	0.0002	29	11	1.55	19.2	27.2
679	2	28	10	1.72	16.9	24.8
679	0.2	28	9	1.44	15.8	23.8
679	0.02	30	11	1.81	16.0	23.9
679	0.002	31	11	1.63	15.4	23.3
679	0.0002	33	13	1.89	15.0	23.0
905	2	28	11	1.73	14.7	22.6
905	0.2	28	8	1.32	13.1	21.0
905	0.02	31	11	1.58	12.8	20.7
905	0.002	34	11	1.48	11.8	19.8
905	0.0002	39	13	1.63	11.1	19.0

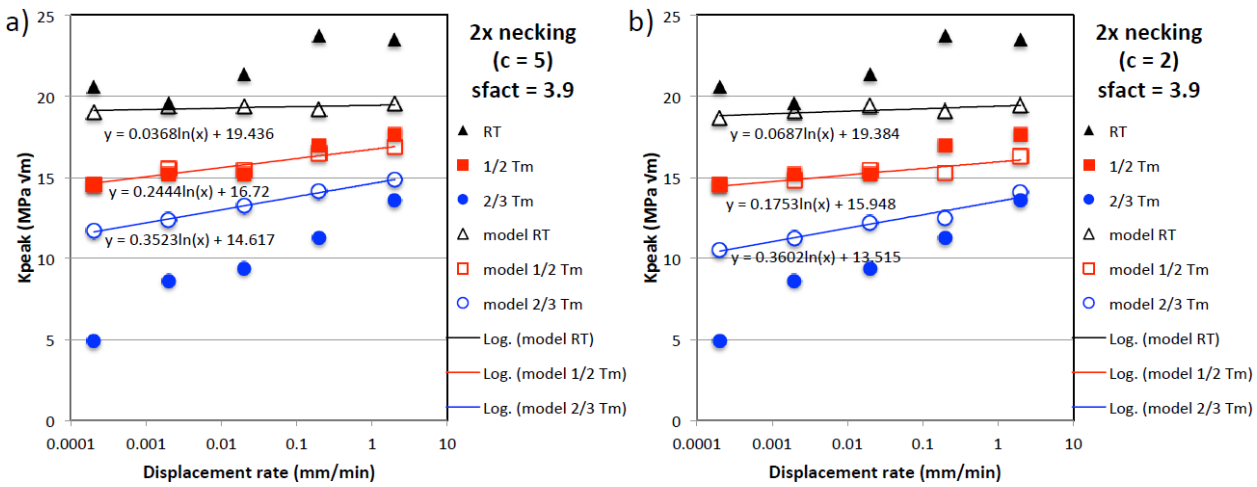

Figure 3. Experimental K_{peak} (filled symbols) and computed a_{Kmax} (open symbols) for W-Cu bridge model vs. displacement rate at room temperature (*RT*), 679 K (*1/2T$_m$*), and 905 K (*2/3T$_m$*). A shift of -6.3 and -8.5 MPa√m is applied to a_{Kmax} data in a) and b) respectively.

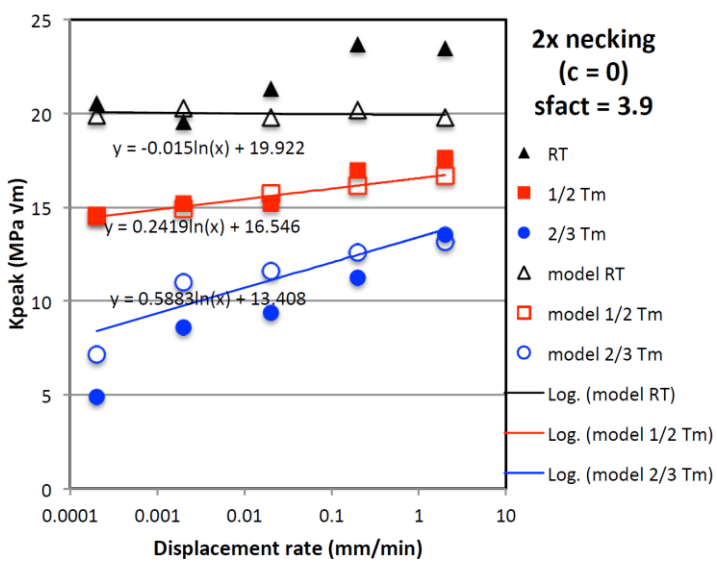

Figure 4. Experimental K_{peak} (filled symbols) and computed a_{Kmax} (open symbols) for W-Cu bridge model vs. displacement rate at room temperature (*RT*), 679 K (*1/2T$_m$*), and 905 K (*2/3T$_m$*). A shift of -12.5 MPa√m is applied to a_{Kmax}.

Discussion

The discrete bridging model described here has been improved to include a more complete treatment of a Cu-bridge in terms of plastic flow as a function of strain rate and temperature, strengthening due to size effects and constraints, and necking with complete control over how the bridges unload and fracture. However, this treatment has some problematic issues associated with it. One is that both strengthening effects and necking effects can be used as adjustable parameters and they appear to provide similar effects on toughening calculations. This makes for difficulties in model validation. Secondly, the comparison with peak load stress intensity, while necessary at this point and convenient, is not as strong a validation test as desired. A better test of the model will be to simulate the load displacement curves as a function of strain rate and temperature. This will also prove challenging given that the observed failure

mode is multiple cracking over a significant plastic zone that is not captured in the model of a single bridged crack. This research will continue to explore model validation and more informative fracture toughness testing, if possible.

References

[1] C. H. Henager, J., R.J. Kurtz, T.J. Roosendaal, B.A. Borlaug, G.R. Odette, K.H. Cunningham, K. Fields, D. Gragg, and F.W. Zok, "Recent Progress in the Development of Ductile-Phase Toughened Tungsten for Plasma-Facing Materials," in Fusion Reactor Materials Program June 30, 2014 DOE/ER-0313/56 – Volume 56, Vol. 56, F. Wiffen, R. Godfrey, and B. Waddell, Editors, 2014, US DOE: ORNL, TN, p. 117-125.

[2] Hollenberg, G.W., G.R. Terwilliger, and R.S. Gordon, "Calculation of stresses and strains in four-point bending creep tests," J. Am. Ceram. Soc., 1971, 54(4), 196-9.

[3] Cox, B.N., "Extrinsic factors in the mechanics of bridged cracks," Acta metallurgica et materialia, 1991, 39(6), 1189-1201.